Energy & Environmental Science

ROYAL SOCIETY OF CHEMISTRY

COMMUNICATION

View Article Online
View Journal | View Issue

Cite this: *Energy Environ. Sci.*, 2020, **13**, 4106

Received 13th August 2020,
Accepted 21st September 2020

DOI: 10.1039/d0ee02585b

rsc.li/ees

A single-component water-lean post-combustion CO_2 capture solvent with exceptionally low operational heat and total costs of capture – comprehensive experimental and theoretical evaluation†

Richard F. Zheng,[a] Dushyant Barpaga,[a] Paul M. Mathias,[b] Deepika Malhotra,[a] Phillip K Koech,[a] Yuan Jiang,[a] Mukund Bhakta,[b] Marty Lail,[c] Aravind V. Rayer,[c] Greg A. Whyatt,[a] Charles J. Freeman,[a] Andy J. Zwoster,[a] Karl K. Weitz[a] and David J. Heldebrant *[a]

A comprehensive evaluation of a recently developed water-lean amine-based solvent, namely *N*-(2-ethoxyethyl)-3-morpholinopropan-1-amine (2-EEMPA), has been performed to analyze its post-combustion CO_2 capture performance. This evaluation comprises (1) fundamental characterization of the solvent–CO_2 interaction using vapor–liquid equilibria, kinetics and viscosity measurements; (2) process characterization of the CO_2 capture performance as measured in a laboratory scale continuous flow system and *via* Aspen Plus® simulation using a flue gas simulant; as well as (3) a full techno economic analysis of the capture process at industrial scale with corresponding projections of critical metrics. This paper summarizes the many parts of this comprehensive evaluation and shows how the various parts come together to empower validated conclusions about its process performance. Notably, it is projected that this solvent can operate at a regeneration heat rate of 2.0 GJ per tonne CO_2 for post-combustion capture, and at a total cost of capture of $50.6/tonne CO_2. With further process optimization significant reductions in the capture cost are predicted.

Broader context

Carbon capture and storage technologies are being pursued to help minimize CO_2 released into the atmosphere, and the related impacts on climate change. The maturity of solvent-based CO_2 separation processes makes them likely to be the first technologies to be implemented at commercial scale for carbon capture. Solvent platforms are also likely the only technologies with robust projections of equipment sizing and cost, due to the existing commercial systems in place for industrial gas separations. Second-generation amine solvents have made meaningful gains in efficiency and reduction in total costs of capture, though still remain prohibitively high. This paper provides a comprehensive experimental and techno-economic assessment of a state-of-the-art single-component water-lean post-combustion carbon capture solvent tested on simulated flue gas. Our analysis demonstrates that this new solvent could lead other solvents in development, with projected regeneration energies and costs lower by 20% and 15%, respectively.

Introduction

Global dependence on coal combustion for power generation, petrochemical processes and related industries continue to emit vast amounts of carbon dioxide (CO_2) per annum into the atmosphere, contributing to worldwide climate change. Emissions reduction *via* post-combustion CO_2 capture can mitigate these adverse environmental effects and has been the focus of recent research and suggested approaches.[1–3] Although modern post-combustion CO_2 capture technology varies, the use of solvents for chemical affinity based capture has matured the most.[4] Amine-based solvents reactive towards CO_2 have shown promising capture performance although many formulations utilize water as a carrier fluid.[5] The presence of this water content in the solvent leads to large energy costs from boiling and condensing required to regenerate the solvent during the continuous capture process.[6,7] Critical metrics for evaluating solvent candidates for this process include operational heat duty, corresponding to the amount of energy required to regenerate the solvent while maintaining stable, continuous capture performance, as well as the cost of CO_2 capture, including both operating and capital costs. Among recent second generation amine solvents that are currently deployed – Mitsubishi Heavy Industries (MHI) solvent, KS-1, and Shell's Cansolv solvent, DC-103 – the operational heat duty reported is

[a] *Pacific Northwest National Laboratory, Richland, USA. E-mail: david.heldebrant@pnnl.gov*
[b] *Fluor Corporation, 3 Polaris Way, Aliso Viejo, CA, 92628, USA. E-mail: Paul.M.Mathias@Fluor.com; Tel: +1-949-349-3595*
[c] *Technology and Commercialization Division, RTI International, Research Triangle Park, NC 27709-2194, USA*

† Electronic supplementary information (ESI) available. See DOI: 10.1039/d0ee02585b

approximately 2.3–2.4 GJ per tonne CO_2[8–10] with a capture cost significantly higher than \$40 per tonne CO_2 target set by the United States Department of Energy.[11]

To this end, water-lean solvent systems have been explored as alternatives to the energy intensive aqueous-amine solvents benefitting from lower specific heats in order to reduce operational heat duty and overall cost of capture.[12] Examples of such systems include task specific ionic liquids,[13,14] phase change materials,[15,16] nanomaterial organic hybrids,[17] aminosilicones,[18,19] siloxylated amine,[20] non-aqueous solvents (NAS),[21–23] and our CO_2-binding organic liquids (CO_2BOLs).[24–26] The complexity of solvent makeup and gas phase analysis associated with multi-component systems as well as the inefficiency in recirculating exogenous co-solvents or diluents have motivated us to focus recent efforts on single-component water-lean capture solvents. Although many similar promising solvent formulations are under development, the lack of comprehensive data needed to assess solvent performance based on those critical metrics for post-combustion CO_2 capture remains a major challenge.

Thus, in this contribution we summarize the comprehensive evaluation of a recently developed water lean solvent, *N*-(2-ethoxyethyl)-3-morpholinopropan-1-amine (2-EEMPA),[27] assessing its CO_2 capture performance based on several experimentally measured datasets. The combination of vapor liquid equilibria, kinetics and solvent viscosity enable understanding of the process aspects and facilitate estimation of process costs through process modeling. We also subjected the solvent to extended exposure with a flue gas simulant in a laboratory-scale continuous flow system (LCFS) to assess its implementation in an industrial process. The combination of LCFS data and corresponding process evaluation *via* Aspen Plus® help characterize the bulk CO_2 capture performance and stability at an applicable scale. Importantly, our techno economic analysis (TEA) projections – which utilize both fundamental and process characterizations – show that implementation of 2-EEMPA in the CO_2 capture process can lower operational heat duty and dramatically reduce total capture cost.

Experimental & modeling methodology

The synthesis and design of the 2-EEMPA solvent was recently reported (Fig. 1) and has been briefly summarized in ESI† Section S1.[27] Experimental data to characterize the solvent performance were collected using a unique, custom "PVT cell" apparatus designed for simultaneous measurement of vapor liquid equilibrium, sorption kinetics and solvent viscosity. Additional details regarding the design and operation of this equipment is described in another contribution, with a summarized methodology provided in the ESI.†[28] Data from the PVT cell were also corroborated using a traditional wetted-wall column (WWC) apparatus.[29] Experimental data to characterize the capture and separation of CO_2 from a flue gas simulant were collected using a laboratory scale sorption/desorption system designed and fabricated in-house, as described in greater detail in this section. The capture and separation performance of the 2-EEMPA solvent was also characterized and compared using simulation by constructing the same experimental sorption/desorption process as an Aspen Plus model, of which basics are also provided in this paper. A more thorough simulation study with corresponding process optimization is planned for future work.

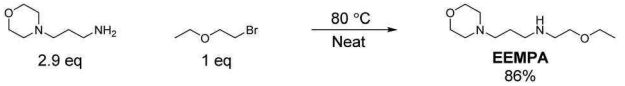

Fig. 1 Synthetic methodology for the synthesis of *N*-(2-ethoxyethyl)-3-morpholinopropan-1-amine (2-EEMPA).

Synthesis

N-(2-Ethoxyethyl)-3-morpholinopropan-1-amine (2-EEMPA) was synthesized in a single step by reaction of the commercially available 3-aminopropylmorpholine and 2-bromoethyl ethyl ether to provide the product in good yields (86%) (Fig. 1). This synthesis of 2-EEMPA was reported recently[27] see ESI† for a detailed procedure (Section S1).

Vapor liquid equilibrium (VLE) measurements

Equilibrium measurements on CO_2 sorption were collected on our PVT cell apparatus based on the static synthetic method,[30] in which known amounts of CO_2 are injected into the cell of known volume and allowed to come to equilibrium pressure at a fixed temperature. It should be noted that our PVT apparatus provides direct measurement of total pressure in the cell. Partial pressure of CO_2 is calculated by taking the difference of this total pressure with the vapor pressure of the solvent at the corresponding temperature. Given the low vapor pressures of the water-lean solvents tested in this system, the total equilibrium pressure is approximately equivalent to the equilibrium partial pressure of CO_2. Thus, the equilibrium pressure can be represented as a function of gas loading to generate isotherms that characterize the performance of the solvent. Additional complementary equilibrium data were also collected using the separate standalone WWC.

Kinetic measurements

Kinetic measurements on CO_2 absorption were also collected using the same PVT cell apparatus that yielded equilibrium measurements. The liquid sample was circulated through an internal WWC with a defined gas/liquid contact area. Instantaneous CO_2 absorption rate data was measured immediately after each CO_2 injection. The liquid film mass transfer coefficient, k_g', was estimated from a regression of the exponential decay of the absorption rate. As with VLE measurements, an additional set of kinetic measurements were also collected using the separate standalone WWC for data quality validation.

Viscosity measurements

Solvent viscosity was also recorded *in situ* during data collection for the VLE and kinetic measurements from the PVT cell apparatus. This was accomplished through a process viscometer (Cambridge ViscoPro 2000) installed in the liquid

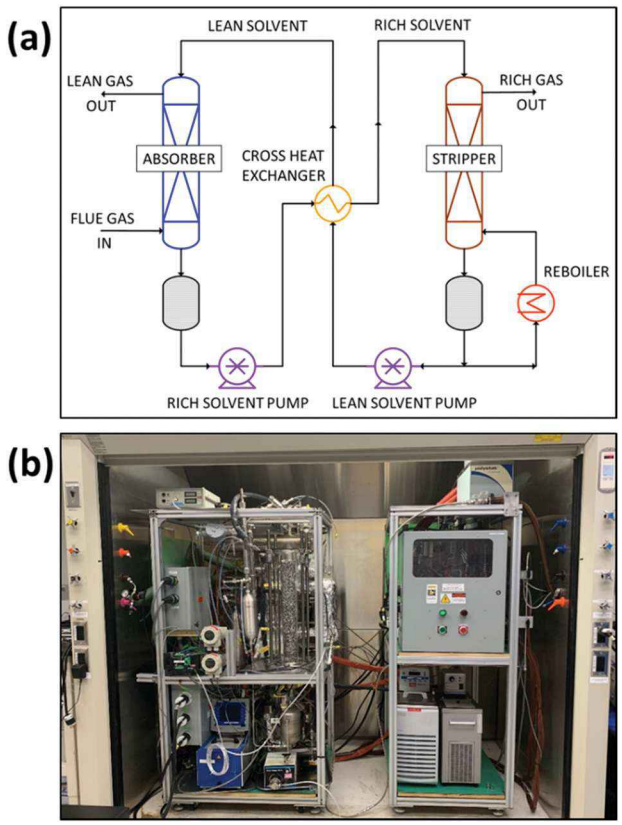

Fig. 2 (a) Basic flow diagram of the LCFS system. Rich/lean designations for both solvent and gas refer to higher/lower concentrations of CO_2, respectively. (b) Photograph of constructed LCFS system designed and operated at PNNL.

recirculation loop to continuously measure viscosity readings of the liquid phase. Viscosity profiles were constructed by averaging the viscosity readings at a given steady state loading.

Continuous capture and separation measurements

The LCFS was designed and constructed based on a typical flowsheet (similar to KM-CDR process developed by Mitsubishi Heavy Industries, Ltd[8]) for the continuous CO_2 capture process (Fig. 2a). This system recirculates a nominal volume of 2-EEMPA between two packed columns as it continuously sorbs and desorbs CO_2 from the flue gas simulant. It is notable that all process equipment and electronics are contained within two mobile carts housed in a walk-in fume hood (Fig. 2b).

In our system, the pre-humidified inlet gaseous stream containing a chosen concentration of CO_2 (see Table 1 for composition) enters the process at the bottom of the absorber column flowing counter currently against the solvent, allowing continuous CO_2 absorption. The lean gas exits the process at the top of the absorber. Lean solvent flow is introduced at the top of the absorber column using an orifice pan liquid distributor equipped with 12 perforated drip tubes. The absorber has a single packing section of 3″ diameter and 20″ height, loaded with a high surface area random packing (0.24″ Pro-Pak 316SS, Canon Instruments). A jacketed glass column vessel is used to control absorber temperature and to observe directly the liquid flow distribution. The LCFS system requires approximately 3–4 L of 2-EEMPA solvent to maintain steady state operations. The CO_2-loaded, rich solvent is then pumped and pre-heated in a brazed plate cross heat exchanger before the stainless steel stripper column (single packing section of 3″ diameter and 24″ height, also loaded with the 0.24″ Pro-Pak packing). A relatively pure CO_2 rich gas stream exits the process after a condenser at the stripper top. The stripper is equipped with a forced convection reboiler. The stripper column also has a heating jacket to counter heat loss on this small column. The hot lean solvent is recirculated back to the absorber after heat recovery using the cross heat exchanger.

The following process variables are controlled during LCFS operation: flue gas flow rate and compositions including water fraction, solvent circulation rate, absorber rich solvent inlet temperature, stripper lean solvent inlet temperature, stripper pressure, reboiler temperature and boil-up ratio. Primary measured variables during operation include lean/rich gas and liquid concentrations and flowrates, which help define the overall capture efficiency of the process. Process temperature, pressure, and CO_2 gas concentration measurements as well as flow and level controls are handed by a custom-built LabVIEW data acquisition and process control system.

The lean and rich gas CO_2 concentrations are analyzed by nondispersive infrared sensors. The CO_2 concentration of the recirculated lean and rich solvent is analyzed by a GC-MS method specifically developed for 2-EEMPA. The water content in the solvent is analyzed by Karl–Fischer titration. Additional details regarding composition analysis are described further in ESI† Section S2.

ASPEN plus model

Rigorous process models for both LCFS and commercial scale processes have developed using rate-based distillation and

Table 1 Composition of flue gas simulants used in the LCFS system as compared to baseline flue gas composition as reported by NETL subcritical case B11A[31]

	Component	Baseline (NETL B11A)	Routine testing	Flue gas simulant
Mole fraction composition (dry gas basis)	N_2	0.8016	0.8493	0.8164
	CO_2	0.1506	0.1507	0.1440
	O_2	0.0380	—	0.0370
	Ar	0.0096	—	0.0026
	SO_2	43.1 ppm	—	4.5 ppm
	NO	60.1 ppm	—	51.9 ppm
Dew point		56 °C	15.6 °C	15.6 °C

other unit-operation models in Aspen Plus®. A thermodynamic package was developed for the 2-EEMPA–H_2O–CO_2 system through the measured data and used in both process models similar to previous modeling efforts.[32] The ElecNRTL-RK property option with reaction stoichiometry, given in eqn (1) and (2), was selected as the base thermodynamic model. The model parameters were regressed using the experimentally measured VLE, kinetic and viscosity data. Reaction kinetics were developed based on the kinetic data. We note that while 2-EEMPA was designed to complex CO_2 as a zwitterionic carbamate[27] the fit of the anhydrous VLE data suggests that the reaction stoichiometry for the anhydrous case is 2 : 1 (*i.e.*, two moles of EEMPA react with one mole of CO_2), thus for this effort we have modeled this as a carbamate reaction. The second reaction models the reaction with water to form the bicarbonate anion. The VLE data indicate that this is a relatively weak reaction. A more detailed analysis of the speciation and stoichiometry will be explored in a future effort.

$$2E + CO_2 \leftrightarrow EH_1^+ + ECO^- \quad (1)$$

$$E + CO_2 + H_2O \leftrightarrow EH_1^+ + HCO_3^- \quad (2)$$

(where E = 2-EEMPA)

In the LCFS process model, the Pro-Pak absorber section was specified according to manufacturer provided data such as specific area, void fraction, and Stichlmair correlation parameters for pressure drop. The packing specific area was scaled from manufacturer data based on the actual packed mass to account for the wall effects of the relatively small diameter of the LCFS absorber column. Key performance measures of LCFS predicted from process model were compared to the performance measures calculated from experimental data.

In the commercial scale process model, the absorber uses Sulzer's Mellapak 250Y packing, while the stripper uses Koch's CMR No. 2 packing. These packing internals were selected based on commercial experience of solvent-based CO_2 capture, and the geometry parameters and other packing specifications are available in the Aspen Plus® database. The plant capacity and flue gas composition were set based on the 550 MW supercritical coal fired power plant with carbon capture designed by NETL.[31] More details about Aspen Plus simulation, and the calculation of mass and energy balances can be found in ESI.†

Techno economic analysis

Techno economic analysis (TEA) was performed for the commercial scale carbon capture process using 2-EEMPA based on the process model developed in Aspen Plus®. The capital costs were estimated by either vendor quote or Aspen Process Economic Analyzer® (APEA). Rigorous TEA with vendor quote was performed for the simple stripper (SS) configuration (as shown in Fig. 2a), while preliminary TEA was also performed for advanced solvent regeneration configurations with capital costs from APEA. Reboiler duty, equivalent work (W_{eq}), net plant efficiency, and cost of carbon capture were identified as the key performance measures to compare 2-EEMPA with other CO_2 capture solvents. 2011 pricing basis was used in the work to be consistent with NETL's reference case.[21] The definition and the approach to calculating these measures can be found in our previous studies and open literature.[31,33,34]

Results and discussion

Fundamental sorption behavior

The experimental characterization of CO_2 sorption equilibrium and kinetics on 2-EEMPA has been summarized in Fig. 3. Equilibrium data are represented using equilibrium CO_2 partial pressure as a function of CO_2 loading (Fig. 3a). As expected, the pressure increases as more gas is loaded onto the solvent. Measurements performed at higher temperatures showed higher overall equilibrium pressures. Solvent viscosities are observed to increase strongly with CO_2 loading (Fig. 3b). As expected, experiments performed at higher temperatures show lower overall solvent viscosities. Sorption kinetics data are represented using the liquid film mass transfer coefficient, k_g', as a function of CO_2 loading (Fig. 3c). The mass transfer coefficient decreases with increasing CO_2 loading and temperatures. This is attributed to differences in the trend of gas solubility with temperature for water-lean solvents.[36,37] This high temperature sensitivity follows previously observed trends for other water-lean CO_2BOL solvents (unlike aqueous amines, where the mass transfer coefficient increases with temperature).[35] It should be noted that analogous equilibrium and kinetics data collected on 2-EEMPA in a WWC apparatus agree well with the data collected on the PVT apparatus, as also shown in Fig. 3. We also note that likely due to larger variations in temperature control at 75 °C (a drift of up to 0.5 °C), the data at low loadings in Fig. 3c shows lower mass transfer coefficients than expected. Thus, a larger experimental error is propagated in the calculation of these points as compared to lower temperature data.

This VLE and kinetics data for 2-EEMPA were also compared with data for monoethanolamine (MEA),[35] a typical reference CO_2 capture solvent as shown in Fig. S4 (ESI†). The underlying assumptions forming the basis of this comparison are outlined in detail in ESI† Section S2. Compared to MEA, and for an absorption process that starts and ends at the same P* swing, the absorption rate of CO_2 by 2-EEMPA was found to be comparable if not faster at least at 40 °C.

Capture performance

The CO_2 capture performance of 2-EEMPA was evaluated experimentally using the LCFS system. For typical industrial operation, the entering flue gas is first passed through a pre-scrubber and/or direct contact cooler to reduce SO_x and NO_x levels and reduce its temperature and water content prior to entering the CO_2 capture unit. In our LCFS system, this has been accounted for by reducing the SO_2 and NO to about 5 ppm and 50 ppm, respectively (Table 1). The flue gas simulant is also pre-humidified to a 15.6 °C dew point to match the process flowsheet's inlet water concentration. This dew point of 15.6 °C

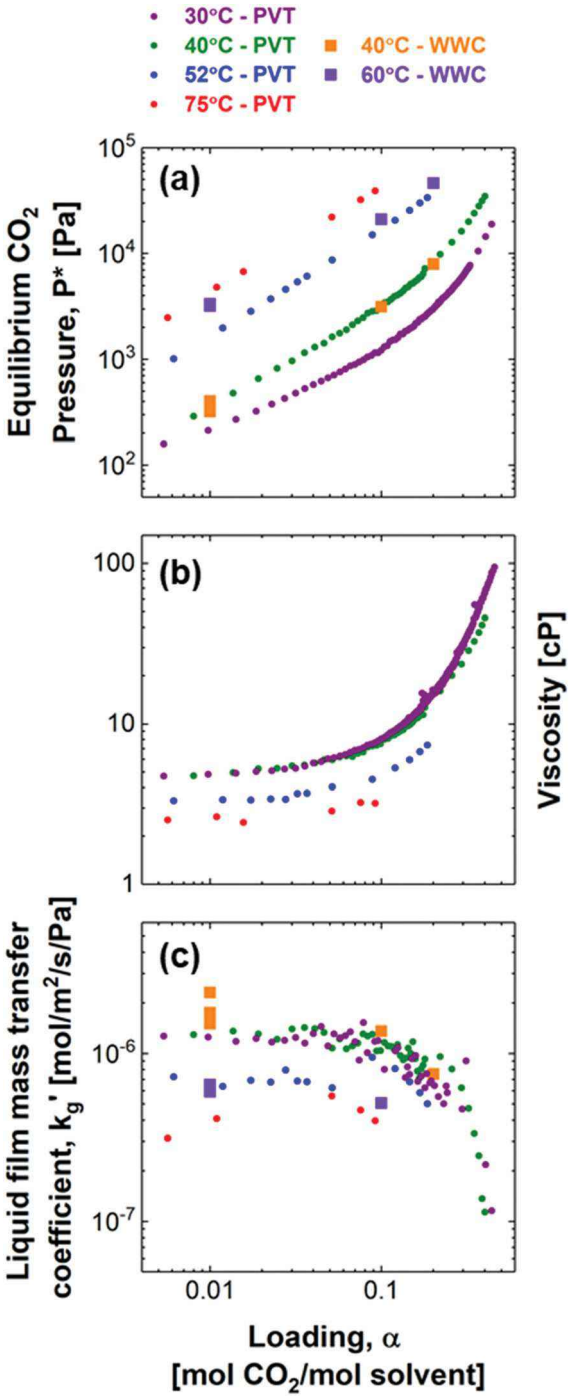

Fig. 3 Representative characterization of (a) vapor liquid equilibrium, (b) solvent viscosity, and (c) absorption kinetics for CO_2 sorption on 2-EEMPA as measured using our PVT cell apparatus. Data quality is corroborated using analogous data collected on a WWC apparatus.

resulted from process design and techno-economic analysis to lower the carbon capture cost. In a commercial scale plant, the flue gas can be cooled to 15.6 °C by using chilling water in the direct contact cooler.

The LCFS was initially started up and operated to steady state with a binary CO_2/N_2 feed gas (Table 1, routine testing composition) for 20 hours, followed by approximately 40 hours at steady state with the simulated flue gas. The purpose of the initial 20 hours of operation with routine gas was to perform system startup and to make sure the 2-EEMPA solvent performance was stable in the absence of oxygen, SO_2, or NO. A snapshot of the relevant process conditions monitored during the course of this operation is shown in Fig. 4. Greater than 95% CO_2 capture was maintained throughout the test duration with the full flue gas simulant composition. It should be noted that due to the relatively short absorber section in this laboratory-scale system, a relatively high L/G ratio of 14.9 (mass basis) was needed. A taller absorber section would have required a lower L/G to achieve a similar capture efficiency, but this had not been the focus of the current evaluation. Variations in water and carbon dioxide as measured *in situ* in the gas phase or by periodical liquid sampling during operation are also shown in Fig. 4. Overall, during the course of the LCFS operation with flue gas simulant, the measured concentrations were steady and within experimental errors. At these particular test conditions, the CO_2 loading in the rich 2-EEMPA was

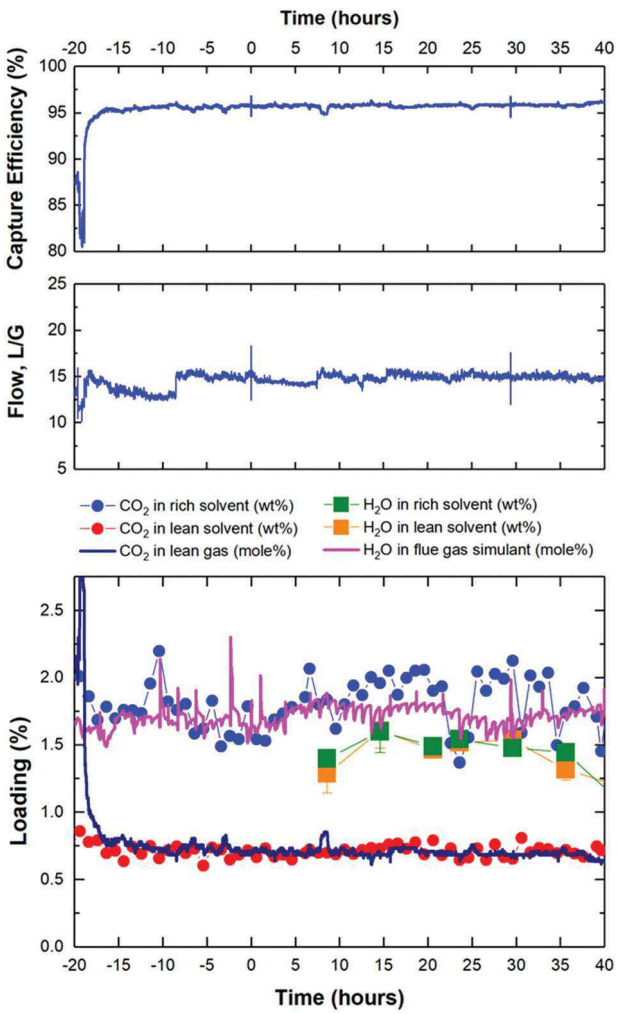

Fig. 4 Monitored process conditions during LCFS testing (absorber feed gas switched from binary CO_2/N_2 mixture to full flue gas simulant at time-on-stream = 0).

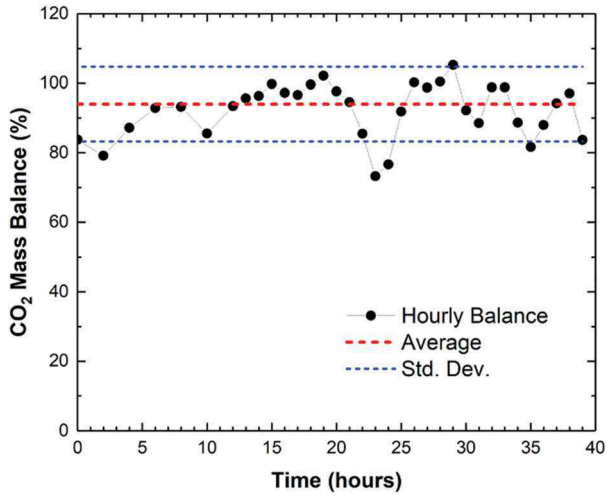

Fig. 5 Hourly CO_2 mass balance during operation of LCFS with flue gas simulant.

observed to be ~1.5–2.0 wt% and in the lean 2-EEMPA it was ~0.75 wt%, while the CO_2 concentration in the treated gas exiting the absorber was at ~0.75 mole%. The steady state water content in the recirculating 2-EEMPA was about 1.5 wt% with the flue gas simulant water content controlled at 15.6 °C dew point (~1.75 mol%).

A mass balance of CO_2 around the absorber was carried out periodically during operation based on flow rate and concentration measurements to validate observed capture performance (Fig. 5). An overall mass balance of 94% was recorded with an error of ±12% propagated from uncertainties in the measured variables. The largest contribution to the slight inaccuracy in mass balance is attributed to the uncertainty in the liquid mass flow. This was because the measured volume flow rate fluctuated within certain bands due to actions of the level controllers. Additionally, liquid density values used in the mass balance calculation were interpolated based on stream temperature and density data from solvent samples without water. The CO_2 mass balance is determined to be adequate.

Quantitative water mass balance was not performed. However, the LCFS test loop is configured such that water can only exit the system with the lean flue gas product stream or the stripper CO_2 rich product stream. Both gas streams were chilled to 16 °C in condensers before venting. The stripper product gas condensate was returned to the lean solvent circulation. The absorber product gas condensate was trapped but only negligible amount of liquid water was collected during operation. The water mass fractions on the circulated solvent remained constant according to Karl–Fischer titration analysis of the solvent samples (Fig. 4). SO_2 and NO mass balance was not attempted due to the trace quantities used. However, no signs of degradation in CO_2 capture performance, solvent visual appearance change, foaming, or solid precipitation were observed when operating with SO_2 and NO in the flue gas simulant.

Capture performance was also evaluated using Aspen Plus simulation of the LCFS test loop and performed at the measured absorber and stream conditions. The simulation results were compared directly with the measured outlet stream properties (Table 2). The measured data is shown to agree well with the simulated properties even though there is uncertainty in the Aspen Plus thermodynamic package as well as in the effective area of the packing section. The largest deviation is in the flue gas outlet CO_2 mole fraction, which is expected given its small absolute value.

Techno economic analysis

Evaluation of CO_2 capture performance *via* TEA allows cost and energetics projections of an industrial scale process using 2-EEMPA. Estimates on key performance and economic metrics of the capture process are shown in Table 3. More details in mass and energy balance, breakdowns of cost and energy consumptions can be found in the ESI.† Rigorous TEA was performed for the simple stripper (SS) configuration to compare 2-EEMPA with commercial solvents, MEA (NETL Case 12)[38] and Cansolv (NETL Case B12B).[31] The SS configuration of the capture process shows significant benefit in replacing Cansolv and MEA with 2-EEMPA. Specifically, the operational reboiler heat duty of 2-EEMPA is 2.27 GJ per tonne CO_2, nearly 30% lower than MEA, and 10% lower than Cansolv. However, because of its relatively high viscosity and solvent circulation rate, the capital cost of 2-EEMPA is slightly higher than Cansolv when considering the same construction material. Consequently, the overall cost of capture of 2-EEMPA is $55.6/tonne CO_2, about 5% lower than Cansolv.

Further improvements to the process were also explored that assess alternate configurations and different material of construction that may impact energetics and cost.[33] These include performing desorption using either a Two-Stage Flash (TSF), an Inter-Heated Column (IHC), an Advanced Heat Integration (AHI) method, Lean-Vapor Compression (LVC) or a combination of several of these options (namely, AHI, IHC, and LVC) instead of a SS.[33,39] In TSF, solvent is regenerated in a high pressure flash drum followed by a low pressure flash drum, to enable CO_2 recovery at higher pressure. In IHC, semi-rich solvent is withdrawn from the middle of the stripper to preheat rich solvent from the absorber. In AHI, low pressure steam is used to preheat the rich solvent, taking advantage of

Table 2 Comparison of LCFS test with Aspen simulation results

Variable	Measured (LCFS)	Modeled (ASPEN)	Deviation
Rich solvent CO_2 loading [mol/mol solvent]	0.0933	0.1026	10%
Rich solvent H_2O loading [mass fraction]	0.0149	0.0139	−6.7%
Dry flue gas out CO_2 concentration [mol fraction]	0.0070	0.0094	34%
CO_2 capture efficiency	95.8%	94.4%	−1.5%

Table 3 Key process and economic performance of 2-EEMPA, MEA[38] and Cansolv.[31] (SS: simple stripper; LVC: lean vapor compression; IHC: inter-heated column; AHI: advanced heat integration method)

	MEA[a]	Cansolv[b]	EEMPA	
NETL reference	Case 12	Case B12B	Case B12B	Case B12B
Configuration	SS	LVC	SS	AHI/IHC/LVC
Process metrics				
Lean loading [mol CO_2/mol solvent]	0.27	—	0.045	0.045
Water loading [wt%]	70	—	1.4	1.4
Regeneration temperature [°C]	115	—	119	113
Equivalent work[c] [kJ_e per mol CO_2]	50.1	39.4	35.2	32.7
Reboiler duty [GJ_e per tonne CO_2]	3.55	248	2.27	2.00
Economic metrics				
Total plant cost [MM$, 2011]	—	632	641	416[c]
Cost of CO_2 capture [$ per tonne CO_2]	—	58.3	55.6	50.6

[a] Performance of MEA was evaluated by NETL using historical economic assumption and 2007 pricing basis, which is significantly different than in this work. [b] Cansolv is a proprietary solvent with limited information available in open literature. [c] The absorber is packed with plastic packing instead of stainless steel packing.

difference in heat capacity between lean and rich solvent. The best modeled configuration is the combination of IHC, AHI and LVC together, of which the preliminary TEA projection is also provided in Table 3. Process flow diagram of this integrated configuration can be found in the ESI.† This configuration projects a reboiler heat duty of 2.0 GJ per tonne CO_2. In addition, the unique wettability property of 2-EEMPA enables the use of plastic packing in the absorber, which can significantly reduce the capital cost. With the lower reboiler duty and the cheaper construction material, the CO_2 capture cost can be further reduced to \$50.6 per tonne CO_2. It should be noted that these estimates are based on the thermodynamic package developed for 2-EEMPA (and utilized in Aspen Plus) *via* experimentally obtained VLE data. The performance of 2-EEMPA can be further improved by optimizing key process design parameters, such as regeneration pressure, and lean loading. Improvements in these measurements and optimization around process design parameters may further improve TEA projections.

Conclusions

In summary, we have developed and demonstrated a complete evaluation of 2-EEMPA as a solvent candidate for CO_2 capture. This evaluation includes fundamental characterization of VLE, experimental and modeling of CO_2 capture as well as techno-economic assessment of the corresponding process flowsheet. Moreover, clear trends for VLE data as a function of temperature are observed, consistent with trends for water-lean solvent systems. Continuous capture experiments using a simulated flue gas on our LCFS system provides evidence of sustainable, steady-state capture efficiencies greater than 90% for over 40 hours. Finally, TEA of key energetics and economic parameters of various capture process configurations project operational reboiler heat duties of only 2.0 GJ per tonne with a corresponding total cost of capture as low as \$50.6 per tonne CO_2. This evaluation highlights and demonstrates the potential impact of using our single-component, water-lean 2-EEMPA solvent for post-combustion CO_2 capture. Further process improvements and optimization are possible as we strive to achieve the \$40/tonne CO_2 target.

Conflicts of interest

There are no conflicts to declare.

Acknowledgements

The authors would like to acknowledge the US Department of Energy Office of Fossil Energy FWP 70924 (managed by NETL) for funding this project and the Pacific Northwest National Laboratory (PNNL) for facilities. The authors would also like to thank Robert Perry for insights into diamine behavior along with Abhoyjit Bhown and Joseph Swisher for insights into modeling and configurations. Battelle proudly operates PNNL for DOE under Contract DE-AC05-76RL01830.

Notes and references

1 D. Aaron and C. Tsouris, *Sep. Sci. Technol.*, 2005, **40**(1–3), 321–348.
2 J. P. Ciferno, T. E. Fout, A. P. Jones and J. T. Murphy, *Chem. Eng. Prog.*, 2009, **105**(4), 33–41.
3 M. Bui, *et al.*, *Energy Environ. Sci.*, 2018, **11**(5), 1062–1176.
4 R. R. Bottoms, *Process for Separating Acidic Gases*, *US Pat.*, 1783901, 1930.
5 G. T. Rochelle, *Science*, 2009, **325**(5948), 1652–1654.
6 D. Adams and J. Davison, Capturing CO_2, IEA Greenhouse Gas R&D Programme Report, 2007.
7 A. Cousins, L. T. Wardhaugh and P. H. M. Feron, *Int. J. Greenhouse Gas Control*, 2011, **5**(4), 605–619.
8 M. Iijima, T. Nagayasu, T. Kamijyo and S. Nakatani, MHI's energy efficient flue gas CO_2 capture technology and large scale CCS demonstration test at coal-fired power plants in USA, 2011, p. 26.
9 G. Rochelle, E. Chen, S. Freeman, D. Van Wagener, Q. Xu and A. Voice, *Chem. Eng. J.*, 2011, **171**(3), 725–733.
10 A. Singh and K. Stéphenne, *Energy Proc.*, 2014, **63**, 1678–1685.

11 R. James, A. Zoelle, D. Keairns, M. Turner, M. Woods and N. Kuehn, *Cost and Performance Baseline for Fossil Energy Plants, Volume 1: Bituminous Coal and Natural Gas to Electricity*, NETL-PUB-22638, 2019.
12 D. J. Heldebrant, P. K. Koech, V.-A. Glezakou, R. Rousseau, D. Malhotra and D. C. Cantu, *Chem. Rev.*, 2017, **117**(14), 9594–9624.
13 M. Ramdin, T. W. De Loos and T. J. H. Vlugt, *Ind. Eng. Chem. Res.*, 2012, **51**(24), 8149–8177.
14 D. C. Cantu, J. Lee, M. S. Lee, D. J. Heldebrant, P. K. Koech, C. J. Freeman, R. Rousseau and V. A. Glezakou, *J. Phys. Chem. Lett.*, 2016, **7**(9), 1646–1652.
15 R. J. Perry, B. R. Wood, S. Genovese, M. J. O'brien, T. Westendorf, M. L. Meketa, R. Farnum, J. Mcdermott, I. Sultanova, T. M. Perry, R. K. Vipperla, L. A. Wichmann, R. M. Enick, L. Hong and D. Tapriyal, *Energy Fuels*, 2012, **26**(4), 2528–2538.
16 D. Malhotra, J. P. Page, M. E. Bowden, A. Karkamkar, D. J. Heldebrant, V. A. Glezakou, R. Rousseau and P. K. Koech, *Ind. Eng. Chem. Res.*, 2017, **56**(26), 7534–7540.
17 K. Y. A. Lin and A. H. A. Park, *Environ. Sci. Technol.*, 2011, **45**(15), 6633–6639.
18 R. J. Perry, T. A. Grocela-Rocha, M. J. O'brien, S. Genovese, B. R. Wood, L. N. Lewis, H. Lam, G. Soloveichik, M. Rubinsztajn, S. Kniajanski, S. Draper, R. M. Enick, J. K. Johnson, H.-B. Xie and D. Tapriyal, *ChemSusChem*, 2010, **3**(8), 919–930.
19 R. J. Perry and J. L. Davis, *Energy Fuels*, 2012, **26**(4), 2512–2517.
20 V. Blasucci, C. Dilek, H. Huttenhower, E. John, V. Llopis-Mestre, P. Pollet, C. A. Eckert and C. L. Liotta, *Chem. Commun.*, 2009, 116–118.
21 M. Lail, J. Tanthana and L. Coleman, *Energy Proc.*, 2014, **63**, 580–594.
22 P. D. Mobley, A. V. Rayer, J. Tanthana, T. R. Gohndrone, M. Soukri, L. J. I. Coleman and M. Lail, *Ind. Eng. Chem. Res.*, 2017, **56**(41), 11958–11966.
23 A. V. Rayer, P. D. Mobley, M. Soukri, T. R. Gohndrone, J. Tanthana, J. Zhou and M. Lail, *Chem. Eng. J.*, 2018, **348**, 514–525.
24 D. J. Heldebrant, C. R. Yonker, P. G. Jessop and L. Phan, *Energy Environ. Sci.*, 2008, **1**(4), 487–493.
25 D. C. Cantu, D. Malhotra, P. K. Koech, D. J. Heldebrant, F. Zheng, C. J. Freeman, R. Rousseau and V. A. Glezakou, *Green Chem.*, 2016, **18**(22), 6004–6011.
26 D. Malhotra, P. K. Koech, D. J. Heldebrant, D. C. Cantu, F. Zheng, V. A. Glezakou and R. Rousseau, *ChemSusChem*, 2017, **10**(3), 636–642.
27 D. C. Cantu, D. Malhotra, P. K. Koech, D. Zhang, V.-A. Glezakou, R. Rousseau, J. Page, F. Zheng, R. J. Perry and D. J. Heldebrant, *ChemSusChem*, 2020, **13**(13), 3429–3438.
28 R. Zheng, D. Barpaga, A. J. Zwoster, P. K. Koech, D. Malhotra and D. J. Heldebrant, 2020, in preparation.
29 D. Roberts and P. V. Danckwerts, *Chem. Eng. Sci.*, 1962, **17**(12), 961–969.
30 R. E. Gibbs and H. C. Vanness, *Ind. Eng. Chem. Fund.*, 1972, **11**(3), 410–413.
31 T. E. Fout, A. Zoelle, D. Keairns, M. Turner, M. Woods, N. Kuehn, V. Shah, V. Chou and L. Pinkerton, *Cost and Performance Baseline for Fossil Energy Plants Volume 1a: Bituminous Coal (PC) and Natural Gas to Electricity Revision 3*, NETL-2015-1723, 2015.
32 P. M. Mathias, K. Afshar, F. Zheng, M. D. Bearden, C. J. Freeman, T. Andrea, P. K. Koech, I. Kutnyakov, A. Zwoster, A. R. Smith, P. G. Jessop, O. G. Nik and D. J. Heldebrant, *Energy Environ. Sci.*, 2013, **6**(7), 2233–2242.
33 Y. Jiang, P. M. Mathias, C. J. Freeman, R. Zheng and D. J. Heldebrant, Techno Economic Analysis of Post-Combustion Carbon Capture with a 3rd Generation Water-Lean Solvent, AICHE Annual Meeting, Paper 57F, Orlando, FL, USA, 2019.
34 Y.-J. Lin and G. T. Rochelle, *Energy Procedia*, 2014, **63**, 1504–1513.
35 R. E. Dugas, *Carbon Dioxide Absorption, Desorption, and Diffusion in Aqueous Piperazine and Monoethanolamine*, PhD thesis, The University of Texas at Austin, 2009.
36 P. M. Mathias, F. Zheng, D. J. Heldebrant, A. Zwoster, G. Whyatt, C. M. Freeman, M. D. Bearden and P. Koech, *ChemSusChem*, 2015, **8**(21), 3617–3625.
37 F. Zheng, D. J. Heldebrant, P. M. Mathias, P. Koech, M. Bhakta, C. J. Freeman, M. D. Bearden and A. Zwoster, *Energy Fuels*, 2016, **30**(2), 1192–1203.
38 J. L. Haslbeck, N. Kuehn, E. G. Lewis, L. L. Pinkerton, J. Simpson, M. J. Turner, E. Varghese and M. C. Woods, *Cost and Performance Baseline for Fossil Energy Plants, Volume 1: Bituminous Coal and Natural Gas to Electricity Revision 2*, NETL-2010-1397, 2010.
39 D. H. Van Wagener and G. T. Rochelle, *Chem. Eng. Res. Des.*, 2011, **89**(9), 1639–1646.